Inorg. Chem. **2002**, *41*, 6432–6439

Aluminum Orthovanadate ($AlVO_4$): Synthesis and Characterization by ^{27}Al and ^{51}V MAS and MQMAS NMR Spectroscopy

Ulla Gro Nielsen,[†] Astrid Boisen,[‡] Michael Brorson,[‡] Claus J. H. Jacobsen,[‡] Hans J. Jakobsen,[†] and Jørgen Skibsted*[,†]

Instrument Centre for Solid-State NMR Spectroscopy, Department of Chemistry, University of Aarhus, DK-8000 Aarhus C, Denmark, and Haldor Topsøe A/S, Nymøllevej 55, DK-2600 Lyngby, Denmark

Received June 14, 2002

Polycrystalline samples of $AlVO_4$ have been prepared by two methods of synthesis and characterized by ^{27}Al and ^{51}V MAS NMR spectroscopy at 14.1 T. The MAS NMR spectra clearly reveal that essentially pure samples with minor impurities of V_2O_5 and alumina have been obtained. From these samples, ^{27}Al quadrupole coupling parameters and isotropic chemical shifts as well as the magnitudes and relative orientations of the ^{51}V quadrupole coupling and chemical shift tensors have been determined with high precision for $AlVO_4$. These data have been obtained from a combined analysis of multiple-quantum (MQ) MAS NMR spectra and MAS NMR spectra of the central and satellite transitions. The ^{27}Al and ^{51}V NMR data show that the asymmetric unit for $AlVO_4$ contains three isolated VO_4 tetrahedra, one pentacoordinated Al site, and two AlO_6 octahedra. This is in agreement with the supposition that $AlVO_4$ is isostructural with $FeVO_4$ and with a recent structure refinement for $AlVO_4$ based on powder X-ray diffraction (XRD) data. The favorable agreement between the refined crystal structure from powder XRD and the NMR parameters is apparent from a convincing correlation between experimental ^{51}V quadrupole tensor elements and calculated ^{51}V electric field gradient tensor elements obtained by the point-monopole approach. An assignment of the ^{27}Al NMR data is obtained from similar calculations of the ^{27}Al electric field gradients and by estimation of the distortion of the AlO_6 octahedra.

Introduction

Vanadium oxides impregnated on the surface of alumina supports are industrially important catalysts used in a number of catalytic reactions including selective oxidation of hydrocarbons.[1−3] Similarly, vanadium oxides on titania supports are used for selective catalytic reduction of NO_x.[4] Such catalysts are of increasing importance in the efforts to efficiently use the limited resources of fossil fuels and to meet environmental legislation. In the optimization of the catalytic properties (e.g., activity, selectivity, and lifetime) for these catalysts and for identification of the active sites on their surfaces, it is of paramount importance to obtain information about the chemical composition and local structure of the vanadium species on the surface. Generally, this information may be achieved by NMR, ESR, Raman, or IR spectroscopy alone or in combination with X-ray diffraction (XRD) or absorption techniques such as EXAFS and XANES.[5] However, most of these methods require the establishment of correlations between structural and spectroscopic parameters in order to obtain structural information about the surface species. These correlations are usually derived from studies of model compounds with known crystal structures including inorganic vanadates and aluminates as well as metalloorganic compounds. Researchers employing solid-state NMR spectroscopy have established a number of relationships between NMR parameters and structural data, for example, between the ^{27}Al isotropic chemical shift ($\delta_{iso}(^{27}Al)$) and the coordination state for Al

* To whom correspondence should be addressed. E-mail: jskib@chem.au.dk. Fax: +45 8619 6199. Phone: +45 8942 3900.
[†] University of Aarhus.
[‡] Haldor Topsøe A/S.

(1) Le Coustumer, L. R.; Taouk, B.; Le Meur, M.; Payen, E.; Guelton, M.; Grimblot, J. *J. Phys. Chem.* **1988**, *92*, 1230.
(2) Eon, J. G.; Olier, R.; Volta, J. C. *J. Catal.* **1994**, *145*, 318.
(3) Khodakov, A.; Olthof, B.; Bell, A. T.; Iglesia, E. *J. Catal.* **1999**, *181*, 205.
(4) Topsøe, N.-Y. *CATTECH* **1997**, *1*, 125.
(5) Dunn, J. P.; Stenger, H. G., Jr.; Wachs, I. E. *Catal. Today* **1999**, *51*, 301.

10.1021/ic0204023 CCC: $22.00
Published on Web 11/07/2002

in inorganic oxides[6−8] and between the ^{51}V chemical shift anisotropy (CSA) and the degree of condensation for the VO_4^{3-} anions in inorganic vanadates.[9−14]

The only stable compound in the $Al_2O_3-V_2O_5$ system is aluminum orthovanadate ($AlVO_4$), and this phase may be considered an important model compound for V−O−Al bonding in relation to studies of vanadia impregnation on alumina surfaces. However, $AlVO_4$ is rather difficult to synthesize which is partly due to the fact that $AlVO_4$ undergoes a peritectic reaction at 765 °C, preventing its synthesis by high-temperature methods.[15] Probably, for this reason, the synthesis of $AlVO_4$ crystals of sufficient size for structure determination by single-crystal XRD has not been reported. Powder XRD studies of $AlVO_4$ have provided the space group (triclinic, $P\bar{1}$, $Z = 6$) and unit cell parameters while IR studies indicate that the structure contains isolated VO_4^{3-} units, AlO_4 tetrahedra, and AlO_6 octahedra.[16,17] Moreover, from a Raman spectroscopic investigation,[18] it was proposed that $AlVO_4$ is isostructural with $FeVO_4$ for which the crystal structure has been reported from single-crystal XRD.[19] Most recently, $AlVO_4$ has been used as a test compound in the evaluation of a new method for structure determination based on simulated annealing combined with nonlinear least-squares Rietveld refinement.[20] Using this method, a powder XRD profile for $AlVO_4$ was refined in the space group $P\bar{1}$, and fractional atomic coordinates were reported.[20] The refined structure (Figure 1), which closely resembles the structure reported for $FeVO_4$, contains three distinct VO_4^{3-} tetrahedra, two AlO_6 octahedra, and a pentacoordinated AlO_5 unit.

In this work, we present new procedures for the synthesis of $AlVO_4$. The resulting polycrystalline samples are characterized by ^{27}Al and ^{51}V MAS and multiple-quantum (MQ) MAS NMR spectroscopy. This includes a precise determination of the ^{27}Al quadrupole coupling parameters and isotropic chemical shifts for three Al sites. Moreover, the magnitudes and relative orientations of the ^{51}V quadrupole coupling and CSA tensors for three VO_4^{3-} tetrahedra in $AlVO_4$ are determined from ^{51}V MAS and triple-quantum (3Q) MAS NMR experiments. Finally, relationships between the $^{27}Al/^{51}V$ NMR data and the proposed structure for $AlVO_4$ from powder XRD are discussed.

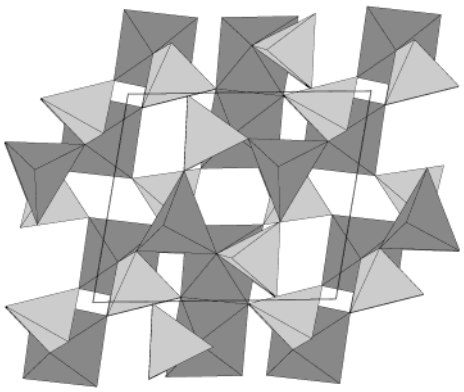

Figure 1. Polyhedral representation of the structure for $AlVO_4$ shown by a projection along the *a* axis and based on the crystallographic data from the refined structure from powder XRD.[20] The light tetrahedra illustrate the isolated VO_4 units while the dark polyhedra show the coordination for aluminum.

Experimental Section

Synthesis of $AlVO_4$. All reagents were of analytical purity grade and were used without further purification. Two samples of $AlVO_4$ were synthesized using the methods described here.

Sample I. A 5.286 g (14 mmol) portion of aluminum nitrate nonahydrate ($Al(NO_3)_3 \cdot 9H_2O$) was mixed with 1.282 g (7.0 mmol) of vanadium(V) oxide (V_2O_5) in a platinum crucible. A 5 mL portion of concentrated nitric acid was added, and the suspension was stirred for 1 h. The suspension was dried for 24 h (110 °C) and subsequently calcined at 650 °C for 5 days.

Sample II. A 3.1965 g (0.0176 mole) portion of V_2O_5 was dissolved in 25 mL of a saturated aqueous solution of tetramethylammonium hydroxide ($(CH_3)_4NOH$). $Al(NO_3)_3 \cdot 9H_2O$ [15.13 g (0.0403 mol)] dissolved in 50 mL of H_2O was slowly added to the vanadium solution. The pH of the resulting solution was adjusted to 14 by adding additional tetramethylammonium hydroxide solution and subsequently filtered. A 6 M solution of HNO_3 was added dropwise to the filtrate until a pH value of 7 was reached. The yellow precipitate was isolated, dried, and finally calcined at 650 °C for 20 h.

NMR Measurements. Solid-state ^{27}Al (156.3 MHz) and ^{51}V (157.7 MHz) MAS NMR experiments were performed at 14.1 T on a Varian Unity INOVA-600 spectrometer using home-built CP/MAS NMR probes for 4 and 5 mm o.d. rotors. The ^{27}Al and ^{51}V single-pulse MAS NMR experiments employed a spectral width of 4 MHz, an rf pulse width of 0.5 μs for $\gamma B_1/2\pi \approx 55$ kHz, and a relaxation delay of 1 s. Baseline distortions were suppressed by linear prediction of the first few data points of the FID followed by baseline correction using the Varian VNMR software. The ^{27}Al and ^{51}V 3QMAS NMR experiments employed a home-built variable-temperature broadband MAS NMR probe for 4 mm o.d. rotors. 3QMAS spectra were acquired using the two-pulse sequence[21] with a 24 step phase-cycling scheme and pulse widths for the 3Q excitation and conversion pulses corresponding to 180° (105°) and 60° (35°) liquid pulses[22] for ^{27}Al (^{51}V), respectively, for an rf field strength of $\gamma B_1/2\pi = 105$ kHz. The indirect dimension was incremented in 128 t_1 steps, and spectral widths of 50 kHz

(6) Müller, D.; Gessner, W.; Behrens, H.-J.; Scheler, G. *Chem. Phys. Lett.* **1981**, *79*, 59.
(7) Smith, M. E. *Appl. Magn. Reson.* **1993**, *4*, 1.
(8) Jansen, S. R.; Hintzen, H. T.; Metselaar, R.; de Haan, J. W.; van de Ven, L. J. M.; Kentgens, A. P. M.; Nachtegaal, G. H. *J. Phys. Chem. B* **1998**, *102*, 5969.
(9) Lapina, O. B.; Mastikhin, V. M.; Shubin, A. A.; Krasilnikov, V. N.; Zamareaev, K. I. *Prog. Nucl. Magn. Reson. Spectrosc.* **1992**, *24*, 457.
(10) Eckert, H.; Wachs, I. E. *J. Phys. Chem.* **1989**, *93*, 6796.
(11) Hayakawa, S.; Yoko, T.; Sakka, S. *Bull. Chem. Soc. Jpn.* **1993**, *66*, 3393.
(12) Skibsted, J.; Jacobsen, C. J. H.; Jakobsen, H. J. *Inorg. Chem.* **1998**, *37*, 3083.
(13) Nielsen, U. G.; Jakobsen, H. J.; Skibsted, J. *Inorg. Chem.* **2000**, *39*, 2135.
(14) Nielsen, U. G.; Jakobsen, H. J.; Skibsted, J. *J. Phys. Chem. B* **2001**, *105*, 420.
(15) Touboul, M.; Popot, A. *J. Therm. Anal.* **1986**, *31*, 117.
(16) Baran, E. J.; Bottom, I. L. *Monatsh. Chem.* **1977**, *108*, 311.
(17) Yamaguchi, O.; Uegaki, T.; Miyata, Y.; Shimizu, K. *J. Am. Ceram. Soc.* **1987**, *70*, C-198.
(18) Hardcastle, F. D.; Wachs, I. E. *J. Phys. Chem.* **1991**, *95*, 5031.
(19) Robertson, B.; Kostiner, E. *J. Solid State Chem.* **1972**, *4*, 29.
(20) Coelho, A. A. *J. Appl. Crystallogr.* **2000**, *33*, 899.
(21) Massiot, D.; Touzo, B.; Trumeau, D.; Coutures, J. P.; Virlet, J.; Florian, P.; Grandinetti, P. J. *Solid State Nucl. Magn. Reson.* **1996**, *6*, 73.
(22) Amoureux, J.-P.; Fernandez, C.; Frydman, L. *Chem. Phys. Lett.* **1996**, *259*, 347.

(^{27}Al) and 150 kHz (^{51}V) were used in both dimensions. All NMR experiments employed exact magic-angle setting and spinning speeds in the range 10−15 kHz with a stability of ±2 Hz, obtained using a Varian Inc. rotor-speed controller. Isotropic ^{27}Al and ^{51}V chemical shifts are relative to a 1.0 M aqueous solution of $AlCl_3 \cdot 6H_2O$ and neat $VOCl_3$, respectively.

Spectral Analysis. Simulations, least-squares fittings, and error analysis of the experimental ^{27}Al and ^{51}V MAS and 3QMAS NMR spectra were performed on a SUN ULTRA-5 workstation using the STARS software package.[23−26] Optimization of integrated to simulated spinning sideband (ssb) intensities for the central and satellite transitions included effects from nonuniform detection (i.e., the quality factor of the probe).[23] Determination of the ^{51}V CSA parameters from the manifolds of ssbs in the isotropic (F1) dimension of the ^{51}V 3QMAS NMR spectra employed the method recently described elsewhere.[27−29] The chemical shift parameters are defined as

$$\delta_{iso} = \frac{1}{3}(\delta_{xx} + \delta_{yy} + \delta_{zz}),\ \delta_o = \delta_{iso} - \delta_{zz},\ \eta_o = \frac{\delta_{xx} - \delta_{yy}}{\delta_o} \quad (1)$$

using the convention $|\delta_{zz} - \delta_{iso}| \geq |\delta_{xx} - \delta_{iso}| \geq |\delta_{yy} - \delta_{iso}|$. The quadrupole coupling parameters (C_Q and η_Q) are related to the principal elements of the electric-field gradient tensor (**V**) by the following equation

$$C_Q = \frac{eQV_{zz}}{h},\ \eta_Q = \frac{V_{yy} - V_{xx}}{V_{zz}} \quad (2)$$

for $|V_{zz}| \geq |V_{xx}| \geq |V_{yy}|$. The relative orientation of the quadrupole coupling and chemical shift tensors is described by the Euler angles ψ, χ, and ξ for $0 \leq \psi \leq 2\pi$ and $0 \leq \chi, \xi \leq \pi/2$,[25] which correspond to positive rotations about δ_{zz} (ψ), the new δ_{yy} (χ), and the final δ_{zz} (ξ) axis.

Results and Discussion

Synthesis. $AlVO_4$ is the only stable compound in the $V_2O_5-Al_2O_3$ system, and the thermodynamic properties described later make synthesis of a pure crystalline sample difficult. Touboul and Popot[15] studied the formation of $AlVO_4$ by differential thermal analysis (DTA) and thermogravimetric analysis (TGA). They observed the crystallization of $AlVO_4$ at 266 °C, an eutectic equilibrium (liquid ↔ $AlVO_4$ + V_2O_5) at 695 °C, and a peritectic equilibrium (liquid + Al_2O_3 ↔ $AlVO_4$) at 765 °C.[15] In a study of $AlVO_4$ solid solutions in the Al_2O_3-rich region of the V_2O_5-Al_2O_3 system, Yamaguchi et al. found that $AlVO_4$ decomposes to V_2O_5 and α-Al_2O_3 when heated above approximately 775 °C.[17] The formation and decomposition of $AlVO_4$, obtained by hydrolysis of a solution containing vanadyl ethoxide and aluminum isopropoxide, were monitored by DTA and powder XRD.[17] Other synthetic methods include approaches similar to the procedure employed in this work for sample I[15,16] and a solution combustion process, where a solution of aluminum nitrate, ammonium metavanadate, ammonium nitrate, and 3-methyl-5-hydrazol is heated rapidly.[30] Method II utilizes the fact that both Al_2O_3 and V_2O_5 are soluble in a strong base. Thus, a solution containing these metals can be prepared. By acidification of such a solution, a precursor material was obtained that upon calcination at 650 °C gave the desired $AlVO_4$ phase free of alkali-ion impurities because tetramethylammonium hydroxide was used as the strong base.

The products resulting from the different methods of synthesis are generally examined by powder XRD[16,17,30] which usually fails to detect amorphous phases. As an example, sample I is observed to be $AlVO_4$ with an impurity of less than 5 wt % V_2O_5 using powder XRD. The V_2O_5 impurity, readily identified by ^{51}V MAS NMR, prevents the determination of precise ^{51}V NMR parameters for $AlVO_4$ because the ssbs from this impurity overlap with one of the manifolds of the ssbs for $AlVO_4$. ^{27}Al MAS NMR spectra of sample I unexpectedly show an additional resonance in the range 45−80 ppm resulting from a minor impurity of amorphous η-alumina; however, this impurity does not affect the analysis of the spectral region for the resonances from $AlVO_4$. With the aim of minimizing the V_2O_5 impurity, a second sample of $AlVO_4$ (i.e., sample II) was synthesized. For this sample, no V_2O_5 impurity could be detected by ^{51}V MAS NMR. However, quite large quantities of alumina impurities, which overlap with the ^{27}Al resonances from $AlVO_4$, are observed by ^{27}Al MAS NMR for sample II. Thus, samples I and II have been used for the ^{27}Al and ^{51}V NMR experiments, respectively. We should note that, despite several attempts, it has not yet been possible to synthesize a completely pure crystalline sample of $AlVO_4$.

^{27}Al MAS and MQMAS NMR. The ^{27}Al MAS NMR spectrum (Figure 2a) of $AlVO_4$ (sample I) is dominated by the central and satellite transitions from a single ^{27}Al site (i.e., Al(1)) influenced by a fairly weak quadrupole coupling. Least-squares optimization of simulated to integrated spinning sideband (ssb) intensities for the satellite transitions for this site leads to determination of precise values for the quadrupole coupling parameters (C_Q and η_Q) and the isotropic chemical shift (δ_{iso}). A simulated spectrum (Figure 2b) based on these parameters (Table 1) reproduces all features in the experimental manifold of ssbs for the Al(1) site. Expansion of the spectral region for the central transitions (Figure 3a) shows a second-order quadrupolar line shape in the region 5−30 ppm, originating from an ^{27}Al site (i.e., Al(2)) with a strong quadrupole coupling. C_Q, η_Q, and δ_{iso} are readily determined for this site by simulation of the second-order quadrupolar line shape. Furthermore, examination of the spectral region from −30 to 0 ppm reveals that the narrow center band for the Al(1) site is superimposed on a much broader resonance, originating from one or more ^{27}Al sites.

(23) Skibsted, J.; Nielsen, N. C.; Bildsøe, H.; Jakobsen, H. J. *J. Magn. Reson.* **1991**, *95*, 88.
(24) Skibsted, J.; Nielsen, N. C.; Bildsøe, H.; Jakobsen, H. J. *Chem. Phys. Lett.* **1992**, *188*, 405.
(25) Skibsted, J.; Nielsen, N. C.; Bildsøe, H.; Jakobsen, H. J. *J. Am. Chem. Soc.* **1993**, *115*, 7351.
(26) Skibsted, J.; Vosegaard, T.; Bildsøe, H.; Jakobsen, H. J. *J. Phys. Chem.* **1996**, *100*, 14872.
(27) Wang, S. H.; Xu, Z.; Baltisberger, J. H.; Bull, L. M.; Stebbins, J. F.; Pines, A. *Solid State Nucl. Magn. Reson.* **1997**, *8*, 1.
(28) Nielsen, U. G.; Jakobsen, H. J.; Skibsted, J. *Solid State Nucl. Magn. Reson.* **2001**, *20*, 23.
(29) Nielsen, U. G.; Jakobsen, H. J.; Skibsted, J. *Solid State Nucl. Magn. Reson.*, in press.
(30) Ekambaram, S.; Patil, K. C. *J. Alloys Compd.* **1995**, *217*, 104.

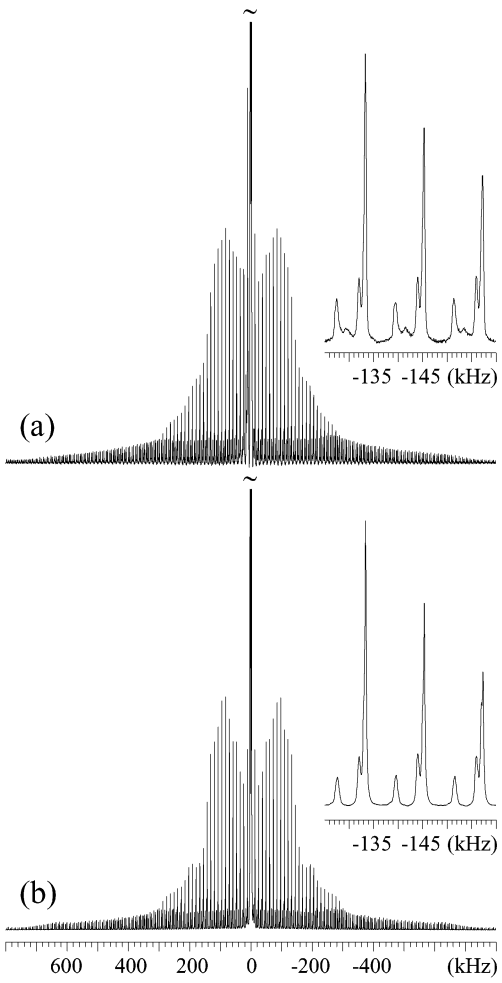

Figure 2. (a) ^{27}Al MAS NMR spectrum (14.1 T, $\nu_r = 12.0$ kHz) of $AlVO_4$ illustrating the manifold of ssbs observed for the satellite transitions. (b) Optimized simulation of the ssbs in part (a) employing the ^{27}Al parameters in Table 1. The right-hand insets show the resolution and line shapes of the individual ssbs for the three ^{27}Al sites in $AlVO_4$. The central transition for the Al(1) site is cut off at 1/10 of its total height in both spectra.

Table 1. ^{27}Al Quadrupole Coupling Parameters (C_Q, η_Q) and Isotropic Chemical Shifts (δ_{iso}) for $AlVO_4$

site[a]	C_Q (MHz)	η_Q	δ_{iso} (ppm)
Al(1)	1.64 ± 0.10	0.30 ± 0.04	-8.9 ± 0.5
Al(2)	6.73 ± 0.10	0.42 ± 0.02	27.2 ± 0.6
Al(3)	5.88 ± 0.10	0.58 ± 0.03	-1.1 ± 1.0

[a] Assignment of the ^{27}Al NMR data to the specific Al sites in the crystal structure from powder XRD[20] (see text).

An improved resolution of these resonances is achieved in the ^{27}Al 3QMAS NMR spectrum of $AlVO_4$ illustrated in Figure 4. The contour plot as well as the isotropic (F1) dimension of this spectrum clearly resolve three resonances for $AlVO_4$. Moreover, a broad, low-intensity resonance is observed at about 5−15 ppm in the F2 dimension which originates from an impurity in the sample. We note that the three ^{27}Al resonances for $AlVO_4$ and the impurity resonance can alternatively be resolved by ^{27}Al MAS NMR at a very high magnetic field (21.15 T) as recently demonstrated.[31] The C_Q, η_Q, and δ_{iso} parameters for the Al(3) site, the site

(31) Nielsen, U. G.; Skibsted, J.; Jakobsen, H. J. *Chem. Commun.* **2001**, 2690.

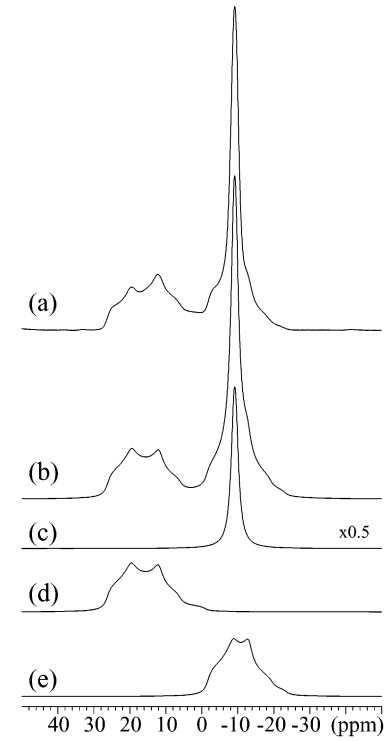

Figure 3. (a) Expansion of the spectral region for the ^{27}Al central transitions observed in the ^{27}Al MAS NMR spectrum of $AlVO_4$ at 14.1 T (cf., Figure 2). (b) Optimized simulation of the central transitions for the three ^{27}Al sites in $AlVO_4$ using the parameters in Table 1. Separate simulations of the second-order quadrupolar line shapes for the individual ^{27}Al sites are shown for Al(1), Al(2), and Al(3) in parts (c), (d), and (e), respectively. The simulated spectra employ the same vertical scale except for the Al(1) site (c) where the vertical scale is reduced by a factor of 2.

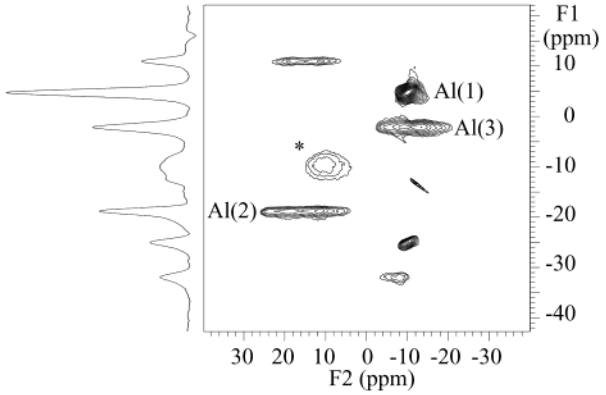

Figure 4. Contour plot for the ^{27}Al 3QMAS NMR spectrum of $AlVO_4$ (14.1 T, $\nu_r = 12.0$ kHz). The contours from the three Al sites in $AlVO_4$ are labeled by Al(1), Al(2), and Al(3) whereas the asterisk indicates the resonance from the impurity phase. The projection onto the F1 axis corresponds to a summation over the 2D spectrum.

overlapping with the Al(1) site in the MAS NMR spectrum (Figure 3a), are determined from line shape analysis of a summation in the F2 dimension over the Al(3) resonance in the 3QMAS spectrum, and they are identical within error limits with the parameters obtained at 21.15 T.[31] The optimized parameters for the three Al sites in $AlVO_4$ are summarized in Table 1 and illustrated by the simulations in Figure 3b−e of the center bands for the central transitions. The total simulation (Figure 3b) reproduces well all features of the experimental spectrum for the central transitions,

except for the region at about 5−15 ppm, where the quadrupolar line shape for the Al(2) resonance is slightly distorted as a result of the overlap with the broad resonance from the impurity phase. The broad and featureless appearance of the resonance from the impurity in the 3QMAS spectrum shows that this resonance originates from an amorphous phase, in agreement with the fact that this impurity is not observed by powder XRD. Furthermore, the estimated chemical shift ($\delta = 10-20$ ppm) demonstrates that the impurity contains aluminum in octahedral coordination. Thus, the impurity is most likely an amorphous alumina phase in our sample I of $AlVO_4$. Using the well-known correlation between $\delta_{iso}(^{27}Al)$ and the Al−O coordination state,[6−8] the resonances for Al(1) and Al(3) are assigned to octahedrally coordinated aluminum, and the resonance from Al(2) is assigned to a pentacoordinated aluminum site. This observation is in agreement with the crystal structure reported by Coelho[20] and thereby supports the expectation that $AlVO_4$ and $FeVO_4$ are isostructural. $AlVO_4$ has earlier been studied by ^{27}Al MAS NMR by Ekambaram and Patil,[30] who only observed a single resonance at 7.1 T. This observation may reflect the fact that the central transitions for the Al(2) and Al(3) sites strongly overlap with the narrow center band from Al(1) in MAS NMR spectra at 7.1 T.[31]

^{51}V MAS and MQMAS NMR. The ^{51}V MAS NMR spectrum ($\nu_r = 10.5$ kHz) of the complete manifold of ssbs from the central and satellite transitions for $AlVO_4$ is shown in Figure 5a. Expansion of the spectral region for the central transitions and of selected ssbs from the satellite transitions (Figure 5a) shows a distinct resolution of resonances from three different vanadium sites. The individual ssbs from the three ^{51}V sites are almost completely separated, a situation which is achieved at 14.1 T only when spinning speeds in the range 10 kHz $\lesssim \nu_r \lesssim$ 11 kHz or above 20 kHz are employed. Obviously, the optimum resolution of the manifolds of ssbs from the three sites is obtained for $\nu_r \gtrsim 20$ kHz; however, for such spinning speeds, the spectral effects from the small ^{51}V CSAs are almost completely eliminated. Furthermore, we note that at 14.1 T the manifolds of ssbs from the satellite transitions for ^{51}V (157.7 MHz) and ^{27}Al (156.3 MHz) overlap only slightly in the outer regions and only for the ^{27}Al and ^{51}V sites with strongest quadrupole coupling. However, at lower magnetic fields, the small difference in Larmor frequencies for ^{51}V and ^{27}Al results in a significant overlap of the ssbs from the satellite transitions for these two spin isotopes which complicates the analysis of the ^{51}V MAS NMR spectra. The manifolds of ssbs for the three ^{51}V sites are observed over a spectral range of 1.2 MHz and are dominated by three intense center bands from the three central transitions. This indicates that the three ^{51}V sites possess moderate-sized quadrupole couplings and small CSAs, which are characteristic features for VO_4^{3-} units in orthovanadates.[12,29] Least-squares fitting of simulated to experimental ssb intensities for the individual manifolds of ssbs, employing the same theoretical approach as used in studies of other inorganic vanadates,[12−14] has been employed for the spectrum in Figure 5a. For one of the ^{51}V sites (i.e., V(2)), this procedure gives a straightforward determination

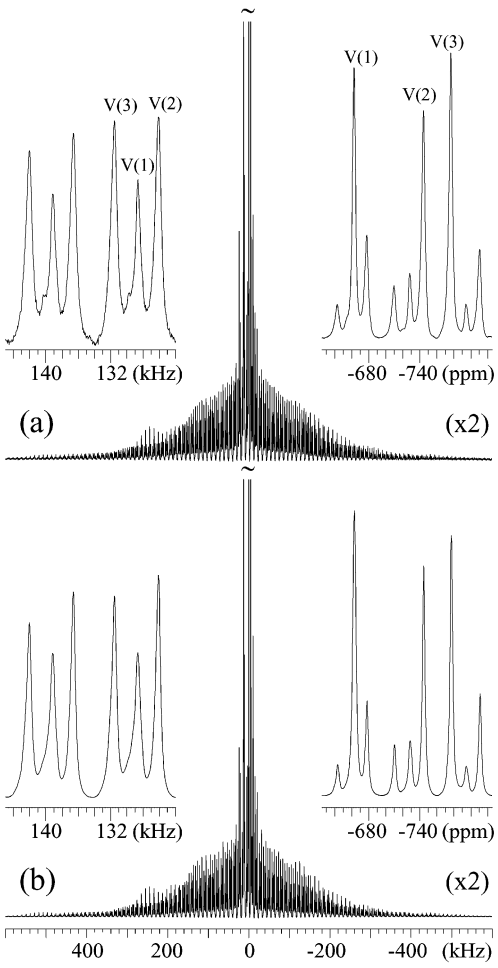

Figure 5. (a) ^{51}V MAS NMR spectrum (14.1 T, $\nu_r = 10.5$ kHz) of the central and satellite transitions for $AlVO_4$ shown on a kilohertz scale relative to the isotropic peak for V(2). (b) Optimized simulation of the three overlapping manifolds of ssbs in part (a) employing the ^{51}V NMR parameters in Table 2 and including second-order quadrupolar effects to account for the line shapes of the ssbs. The right-hand insets show the spectral region for the isotropic peaks (on a ppm scale relative to $VOCl_3$) while the left-hand insets illustrate that the ssbs from the satellite transitions are almost completely separated for the three ^{51}V sites.

of the quadrupole coupling and CSA (δ_σ and η_σ) parameters as well as the Euler angles (ψ, χ, and ξ), relating the principal axis systems for the two tensorial interactions. However, for the manifolds of ssbs from the V(1) and V(3) sites, the least-squares fitting arrives at a minimum in the rms function for two parameter sets corresponding to identical C_Q, η_Q, and η_σ values but δ_σ parameters with opposite sign and different values for the Euler angles. A similar ambiguity in the determination of the sign for the δ_σ parameter has recently been observed for $LaVO_4$.[29] In that work, a reliable determination of δ_σ was obtained by analysis of the ssb manifold observed in the isotropic dimension of a ^{51}V 3QMAS NMR spectrum, utilizing the fact that the CSA interaction is magnified by a factor of 3 in this dimension. The same approach is used here employing the ^{51}V 3QMAS NMR spectrum shown in Figure 6. The ^{51}V 3QMAS NMR spectrum of $AlVO_4$ is dominated by the manifolds of ssbs originating from the three center bands in the isotropic dimension. However, ssb manifolds of lower intensity are also observed for the first-order ssbs in the isotropic

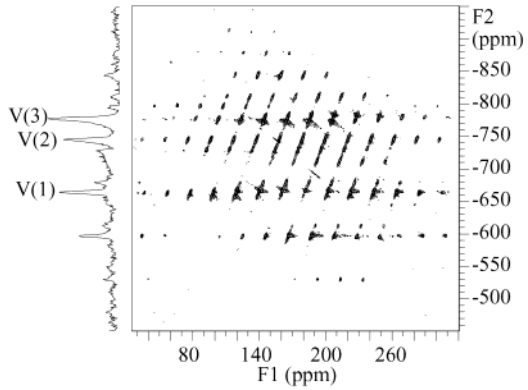

Figure 6. Contour plot of the ^{51}V 3Q MAS NMR spectrum of $AlVO_4$ (14.1 T, $\nu_r = 10.5$ kHz). The projection onto the anisotropic dimension (F2) is a summation. V(1), V(2), and V(3) indicate the isotropic peaks in this dimension for the three ^{51}V sites.

dimension. A reconstruction of these ssb manifolds in the isotropic dimension, employing the approach by Wang et al.,[27] gives subspectra for the three ^{51}V sites that are strongly dominated by the CSA interaction. Including effects from only the CSA interaction in least-squares fits to these subspectra gives an unambiguous determination of the sign for δ_σ as well as the magnitudes for δ_σ and η_σ for the V(1) and V(3) sites (cf., Table 2). It is noted that the CSA parameters cannot be determined in a similar manner for the V(2) site, because the small quadrupole coupling for this site ($C_Q = 2.35$ MHz) results in modulations of the first-order quadrupole coupling interaction which significantly contribute to the ssb intensities in the isotropic dimension.[32] The CSA data determined from the 3QMAS spectrum are subsequently used as fixed parameters in least-squares optimizations for the determination of the ψ, χ, and ξ Euler angles from the manifolds of ssbs for the V(1) and V(3) sites in the ^{51}V MAS NMR spectrum (Figure 5a).

The analysis described here gives the magnitudes and relative orientations of the quadrupole coupling and CSA tensors for the three ^{51}V sites in $AlVO_4$ listed in Table 2, which should be considered the optimum data resulting from the combined analysis of the ^{51}V 3QMAS and MAS NMR spectra. The optimized parameters are illustrated by a total simulation (Figure 5b) of the three overlapping manifolds of ssbs and by the simulated spectra for the individual ^{51}V sites illustrated in Figure 7. Eckert and Wachs[10] have earlier studied $AlVO_4$ by ^{51}V MAS NMR at 7.1 and 11.7 T. Although the strong overlap of ssbs for the central transitions from the three ^{51}V sites prevented a determination of the CSA parameters, they reported δ_{iso} values of -661, -745, and -775 ppm for the three sites from analysis of the centers of gravity for the central transitions at the two magnetic fields. These isotropic chemical shifts are in excellent agreement with those determined in this work (cf., Table 2). $AlVO_4$ has most recently been investigated by Kalinikin et al.[33] who reported an estimate of the magnitude of the CSA interaction corresponding to $\Delta\delta \approx 100$ ppm for all three vanadium sites from ^{51}V MAS NMR at 9.4 T; however, no quadrupole coupling parameters were determined. In addition, they reported isotropic chemical shift values of -661, -740, and -772 ppm, in good agreement with those given in Table 2.

Relationships between the ^{27}Al and ^{51}V NMR Parameters and Structural Data. The ^{51}V NMR data for $AlVO_4$ (Table 2) show that each of the three ^{51}V sites possesses small chemical shift anisotropies ($|\delta_\sigma| \approx 80-120$ ppm), $\eta_\sigma \approx 0.7-0.9$, and fairly small quadrupole couplings. Furthermore, the Euler angles (ψ, χ, and ξ) are identical within error limits for the three ^{51}V sites. Nearly identical values for δ_σ, η_σ, and χ have recently been observed for ^{51}V in isostructural ortho-, pyro-, and metavanadates.[12-14] Thus, the similarity of these parameters for $AlVO_4$ shows that the environments of the VO_4^{3-} anions are quite similar for this compound. Moreover, a comparison of the CSAs and quadrupole couplings with those reported for ortho-, pyro-, and metavanadates[9-14] strongly suggests that $AlVO_4$ contains three orthovanadate units (i.e., isolated VO_4^{3-} tetrahedra), in agreement with the refined crystal structure from powder XRD.[20]

Relationships between the ^{51}V data and the refined crystal structure are further investigated by estimation of the ^{51}V electric field gradients (EFGs) using point-monopole calculations in combination with the structural data from powder XRD. These types of calculations, which also have been used in the analysis of ^{23}Na and ^{133}Cs quadrupole coupling parameters,[26,34] have recently proven useful in the assignment of ^{51}V NMR data to specific vanadium sites for pyro- and metavanadates containing multiple ^{51}V sites.[13,14,35] In the approach used in these studies, the point-monopole calculations only consider the oxygen atoms within the first coordination sphere of the V^{5+} ion and employ effective charges for these anions obtained as $q_{eff} = (-2 + \Sigma f_{ij})e$. Here, f_{ij} is the covalence of the oxygen(i)$-$cation(j) bond calculated from the bond-valence equations of Brown and Shannon[36] and the chemical-bond data of Brown and Altermatt.[37] This procedure and the structural data from powder XRD[20] give the calculated ^{51}V EFG tensor elements listed in Table 3 for $AlVO_4$. The calculated EFG elements are correlated with the principal elements of the ^{51}V quadrupole coupling tensors, derived from C_Q and η_Q in Table 2 according to

$$Q_{zz}^{exp} = C_Q,\ Q_{yy}^{exp} = -\frac{1}{2}(1 - \eta_Q)C_Q,\ Q_{xx}^{exp} = -\frac{1}{2}(1 + \eta_Q)C_Q \quad (3)$$

and assuming $C_Q > 0$. The plot of the experimental quadrupole tensor elements as a function of the calculated principal elements of the ^{51}V EFG tensors (Figure 8) demonstrates a linear correlation between these parameters.

(32) Marinelli, L.; Frydman, L. *Chem. Phys. Lett.* **1997**, *275*, 188.
(33) Kalinkin, P.; Kovalenko, O.; Lapina, O.; Khabibulin, D.; Kundo, N. *J. Mol. Catal. A* **2002**, *178*, 173.
(34) Koller, H.; Engelhardt, G.; Kentgens, A. P. M.; Sauer, J. *J. Phys. Chem.* **1994**, *98*, 1544.
(35) Nielsen, U. G.; Jakobsen, H. J.; Skibsted, J.; Norby, P. *J. Chem. Soc., Dalton Trans.* **2001**, *21*, 3214.
(36) Brown, I. D.; Shannon, R. D. *Acta Crystallogr., Sect. A* **1973**, *29*, 266.
(37) Brown, I. D.; Altermatt, D. *Acta Crystallogr., Sect. B* **1985**, *41*, 244.

Table 2. ^{51}V Quadrupole Coupling (C_Q, η_Q), Chemical Shift Parameters (δ_σ, η_σ, δ_{iso}), and Relative Orientation (ψ, χ, ξ) of the Two Tensors for the ^{51}V Sites in $AlVO_4$[a]

site[a]	C_Q (MHz)	η_Q	δ_{iso} (ppm)	η_σ	ψ (deg)	χ (deg)	ξ (deg)	δ_{iso} (ppm)
V(1)	4.05 ± 0.05	0.84 ± 0.02	87 ± 8	0.74 ± 0.17	114 ± 30	29 ± 23	88 ± 31	−660.5 ± 1
V(2)	2.35 ± 0.03	0.93 ± 0.02	−120 ± 6	0.72 ± 0.10	137 ± 30	27 ± 7	58 ± 30	−743.6 ± 1
V(3)	3.08 ± 0.02	0.62 ± 0.02	−82 ± 7	0.88 ± 0.11	130 ± 30	25 ± 12	15 ± 20	−775.7 ± 1

[a] For a definition of the ^{51}V NMR parameters, see the Experimental Section. [b] Assignment of the ^{51}V NMR parameters to the specific ^{51}V sites in the crystal structure from powder XRD[20] based on calculated ^{51}V EFG tensor elements (see text).

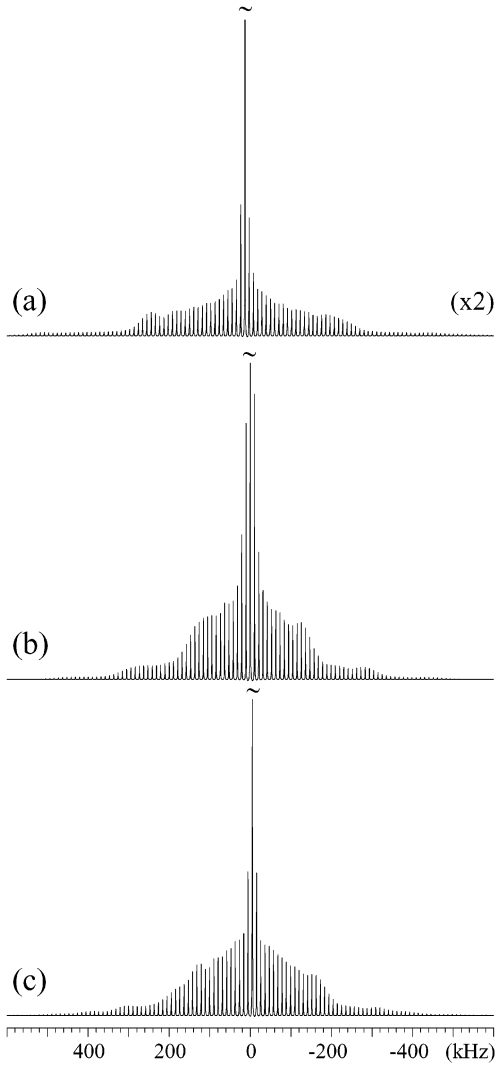

Figure 7. Simulated ^{51}V MAS NMR spectra (14.1 T, ν_r = 10.5 kHz) illustrating the individual manifold of ssbs for the (a) V(1), (b) V(2), and (c) V(3) sites in $AlVO_4$ and corresponding to the optimized ^{51}V parameters in Table 2. Summation of the manifolds of ssbs in parts (a), (b), and (c) gives the simulated spectrum for $AlVO_4$ shown in Figure 5b. All spectra are shown on the same vertical scale; however, the center band for the V(1) site is cut off at half-height.

Linear regression analysis of the data in Figure 8 gives the equation

$$Q_{ii}^{exp} = 3.33V_{ii}^{calc}(10^{20}\ V\ m^{-2}) \quad (4)$$

with the correlation coefficient R = 0.991. The excellent correlation between Q_{ii}^{exp} and V_{ii}^{calc} shows that the ^{51}V quadrupole coupling parameters (Table 2) are in favor of the overall structure reported from powder XRD. Furthermore, the correlation provides an assignment of the ^{51}V NMR parameters in Table 2 to the specific crystallographic vanadium positions in the crystal structure for $AlVO_4$ reported from powder XRD.[20] However, the coefficient of 3.33 relating the EFG tensor to the quadrupole coupling tensor deviates somewhat from the corresponding coefficients determined for divalent metal pyrovanadates (2.34)[14] and metavanadates (2.45).[13] Employing the previously reported ^{51}V quadrupole coupling parameters for the orthovanadates $Mg_3(VO_4)_2$, $Zn_3(VO_4)_2$, $BiVO_4$, and $LaVO_4$[12,29] gives a linear correlation between the experimental quadrupole coupling tensor elements and the calculated principal elements of the ^{51}V EFG tensors corresponding to the equation

$$Q_{ii}^{exp} = 2.46V_{ii}^{calc}(10^{20}\ V\ m^{-2}) \quad (5)$$

with the correlation coefficient R = 0.98. The coefficient in eq 5 is in excellent agreement with those determined for the divalent metal pyro- and metavanadates, considering the simplicity of the point-monopole approach. The larger value observed for $AlVO_4$ (eq 4) may reflect the fact that the refined structure by Coelho[20] gives V−O bond distances which are either shorter or longer than those reported for the VO_4 tetrahedra in the isostructural compound $FeVO_4$.[19] For example, the refined structure of $AlVO_4$ gives V−O bond distances of 1.56, 1.59, 1.80, and 1.82 Å for the V(1) site

Table 3. Calculated Principal Elements ($\mathbf{V}_{ii}^{calc}$)($\times 10^{20}$ V m^{-2}) of the ^{51}V Electric Field Gradient Tensors for the Vanadium Sites in $AlVO_4$[a]

site[a]	V_{xx}^{calc}	V_{yy}^{calc}	V_{zz}^{calc}
V(1)	−1.066	−0.237	1.301
V(2)	−0.644	−0.048	0.692
V(3)	−0.772	−0.147	0.919

[a] Calculated values from point-monopole calculations (see text) using the structural data reported from powder XRD.[20]

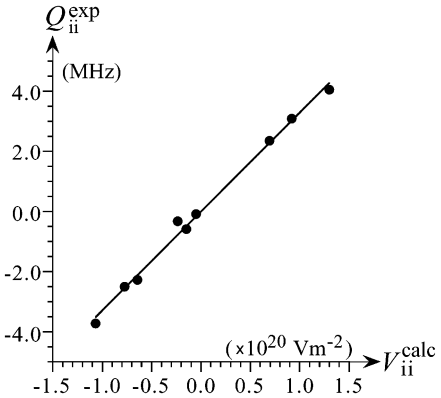

Figure 8. Linear correlation between the ^{51}V quadrupole coupling tensor elements (Q_{ii}^{exp}) and calculated EFG tensor elements (V_{ii}^{calc}) from point-monopole calculations (Table 3) for the three ^{51}V sites in $AlVO_4$. The straight line shows the results of linear regression (cf., eq 4).

whereas the corresponding distances for the V(1) site in $FeVO_4$ are 1.65, 1.66, 1.78, and 1.79 Å. These bond lengths for $FeVO_4$ are very similar to those determined for VO_4 tetrahedra in other orthovanadates whereas the V−O bond distances for $AlVO_4$ deviate significantly from these values. This indicates that the atomic coordinates determined for $AlVO_4$ from powder XRD are not as accurate as those reported for $FeVO_4$ from single-crystal diffraction. Recently, we have observed that precise structural parameters are required to obtain a reliable correlation between ^{51}V quadrupole coupling tensors and calculated ^{51}V EFG tensors.[35] Thus, we expect that the difference in coefficients in eqs 4 and 5 indicates that the structural data reported for $AlVO_4$ are of lower precision as compared to the single-crystal XRD structures reported for $FeVO_4$ and for the orthovanadates $Mg_3(VO_4)_2$, $Zn_3(VO_4)_2$, $BiVO_4$, and $LaVO_4$. Thus, eq 5 represents an improved correlation between ^{51}V quadrupole coupling tensor elements and calculated principal elements of the ^{51}V EFG tensors for orthovanadates as compared to the correlation (eq 4) observed for $AlVO_4$.

An assignment of the ^{27}Al resonances to the specific crystallographic sites in the powder XRD structure is obtained from similar point-monopole calculations of the ^{27}Al EFGs. The ^{27}Al resonance with $\delta_{iso} = 27.2$ ppm originates from a pentacoordinated Al site, and thus, this resonance is assigned to the Al(2) site in the crystal structure of Coelho.[20] Point-monopole calculations of the ^{27}Al EFGs for Al(1) and Al(3) give the unique EFG tensor elements $V_{zz}^{calc} = 0.70 \times 10^{20}$ V m^{-2} and $V_{zz}^{calc} = 1.48 \times 10^{20}$ V m^{-2}, respectively. Thus, the ^{27}Al resonances with quadrupole couplings $C_Q = 1.64$ MHz and $C_Q = 5.88$ MHz are assigned to the Al(1) and Al(3) sites, respectively, in the crystal structure from powder XRD.[20] Alternatively, the distortion of the AlO_6 octahedra can be described by the mean deviation (D) of the O−Al−O bond angles (θ_i) from the ideal value ($\theta_o = 90°$ or 180°) for a perfect octahedron defined by

$$D = \frac{1}{15}\sum_{i=1}^{15}|\theta_i - \theta_o| \qquad (6)$$

This parameter has earlier been employed in interpretations of ^{17}O and ^{27}Al quadrupole coupling constants,[38,39] assuming that increasing D is reflected by an increase in C_Q. Calculation of D for the two octahedrally coordinated Al sites in the structure from powder XRD gives the values $D = 4.9°$ and $D = 7.0°$ for Al(1) and Al(3), respectively. Thus, this approach results in the same assignment of the ^{27}Al NMR resonances as obtained by the point-monopole calculations.

Conclusions

Polycrystalline samples of $AlVO_4$, containing only small quantities of V_2O_5 and alumina impurities, have been prepared using two different methods of synthesis. The characterization of these samples by ^{27}Al and ^{51}V MAS NMR of the central and satellite transitions and by MQMAS NMR has shown that the asymmetric unit for $AlVO_4$ includes three isolated VO_4 tetrahedra, one pentacoordinated Al site, and two AlO_6 octahedra. These observations support the supposition that $AlVO_4$ and $FeVO_4$ are isostructural compounds and are in agreement with the refined crystal structure for $AlVO_4$ from powder XRD.[20] The MAS and MQMAS NMR spectra have allowed the determination of precise values for the anisotropic parameters characterizing the ^{27}Al quadrupole couplings and the magnitudes and relative orientations of the ^{51}V quadrupole coupling and chemical shift tensors. These parameters have been assigned to the specific Al and V sites in the crystal structure obtained from powder XRD, employing point-monopole calculations of the ^{51}V and ^{27}Al electric field gradient tensors. A convincing correlation between these calculated data and the experimental elements for the ^{51}V quadrupole coupling tensors illustrates an excellent coherence between the proposed crystal structure from powder XRD[20] and the NMR data determined in this work.

Acknowledgment. The use of the facilities at the Instrument Centre for Solid-State NMR Spectroscopy, University of Aarhus, sponsored by the Danish Natural Science Research Council, the Danish Technical Science Research Council, Teknologistyrelsen, Carlsbergfondet, and Direktør Ib Henriksens Fond, is acknowledged. J.S. thanks the Danish Natural Science Research Council for financial support (J. No. 0001237).

Supporting Information Available: Crystallographic data in CIF format. This material is available free of charge via the Internet at http://pubs.acs.org.

IC0204023

(38) Turner, G. L.; Chung, S. E.; Oldfield, E. *J. Magn. Reson.* **1985**, *64*, 316.
(39) Skibsted, J.; Henderson, E.; Jakobsen, H. J. *Inorg. Chem.* **1993**, *32*, 1013.